PARAMETER STUDY FOR POLYMER SOLAR MODULES BASED ON VARIOUS CELL LENGTHS AND LIGHT INTENSITIES

L.H. Slooff[1], A.R. Burgers[1], E.E. Bende[1], S.C. Veenstra[2], J.M. Kroon[1]
[1]ECN Solar Energy, P.O. Box 1, 1755 ZG Petten, The Netherlands
[2]ECN Solar Energy, Solliance, High Tech Campus 5 (P63), 5656AE Eindhoven, The Netherlands
Phone: +31 88 515 4314, Fax: +31 88 515 8214, E-mail: slooff@ecn.nl

ABSTRACT: Polymer solar cells may be applied in portable electronic devices, where light intensity and spectral distribution of the illuminating source can be very different compared to outdoor applications. As the power output of solar cells depends on temperature, light intensity and spectrum, the design of the module must be optimized for the specific illumination conditions in the different applications. The interconnection area between cells in a module must be as narrow as possible to maximize the active area, also called geometrical fill factor, of the module. Laser scribing has the potential to realize this. The optimal width of the interconnection zone depends both on technological limitations, e.g. laser scribe width and the minimal distance between scribes, and electrical limitations like resistive losses. The latter depends on the generated current in the cell and thus also on illumination intensity. Besides that, also the type of junction, i.e. a single or tandem junction, will influence the optimal geometry. In this paper a calculation model is presented that can be used for electrical modeling of polymer cells and modules in order to optimize the performance for the specific illumination conditions.
Keywords: Organic Solar Cell, Modelling, Electrical Properties, Metallization

1 INTRODUCTION

Polymer solar cells show a steadily increasing power conversion efficiency which has recently reached values of over 10% for sizes up to 1 cm^2 [1,2]. One of the promising application areas of these type of cells are as an energy generating unit in portable electronic devices. In these applications, the polymer solar cells will face different spectral and light intensity conditions. Both these factors will influence the efficiency of the solar cell [3,4]. Modern indoor light sources are optimized to the response of the human eye. As a result, the irradiance spectra of these sources covers the visible part of the spectrum, not the infra-red. These irradiance spectra match very well with the spectral response of most organic photovoltaic (OPV) cells, thereby increasing the efficiency. Secondly, when light intensities are low, resistive losses will be lower. For this reason, the design of the cells must be optimized for the specific light conditions that occur for a specific application. This is where modeling can play an important role.

Device physics and optical models have been reported [5-9] that accurately describe the observed device performance on cell level. These models describe the intrinsic cell performance, i.e. they do not take into account the effects of series resistance caused by the metallization and external circuit. Such device physics and optical modeling can be used to determine the accurate device structure with respect to layer thicknesses in the device.

Optimization of the metallization for the electrodes has been reported by several groups [10,11]. All these models need an intrinsic current-voltage (I-V) characteristics as input, to describe the diode characteristics of the cell. This can be based on an experimental I-V curve which has been corrected for the series resistance and shadow losses in the measurement (intrinsic I-V curve), or it can be the result of a device physics model. Finite element modeling (FEM) has been used to describe the performance for grid based cells with different cell lengths and finger pitch [12].

Here we report on a FEM model that takes into account the cell and interconnection of a grid based thin film cell. The intrinsic I-V curve is fitted to a 1-diode model and the resulting cell parameters are used as input for the model together with the resistances of the various layers. Calculations are presented for polymer P3HT:[C60]PCBM cells with different grid patterns and for varying cell lengths. First calculations are done for a cell structure with ITO as the transparent electrode (TE) and a composite electrode consisting of PEDOT and ink jet printed (IJP) lines. Next the ITO is replaced by a TE with 10 and 100 times lower sheet resistance. Then also the line resistance and resistance in the contact of the interconnection are varied. Finally it is show that the light intensity influences the optimal electrode structure.

2 APPROACH

2.1 The interconnection model

A finite element model was developed that describes the thin film solar cell and its metal contacts as well as the interconnection from the top contact of one cell to the back contact of the next cell in a module. In this paper we refer to this as a single cell module. A schematic presentation of the device layout is shown in Fig.1. The model is based on monolithic interconnection of individual cells using scribes for the isolation between the photoactive layer and the metal of the interconnection (P1), between the metal of the interconnection and the photoactive layer of the next cell (P3) and to open the way for the metal contact between the front side of one cell and back side of the other cell (P2). In principle other configurations can be calculated as well, but will not be addressed here.

In the model it is assumed that the isolation scribe (P1) is good enough so that there will be no direct current flow between the active layer and the metal of the interconnection. For this reason the isolation and photo-active material between the isolation and the metal of the interconnection were omitted in the model. In this way the device can be treated as a quasi 2-dimentional system.

The model cell contains several layers: the top metal grid, the active layer and the back contact layer. The active layer is described by a 1-diode equation with its diode parameters, photocurrent density (J_{ph}), dark saturation current density (J_0), diode ideality factor (n),

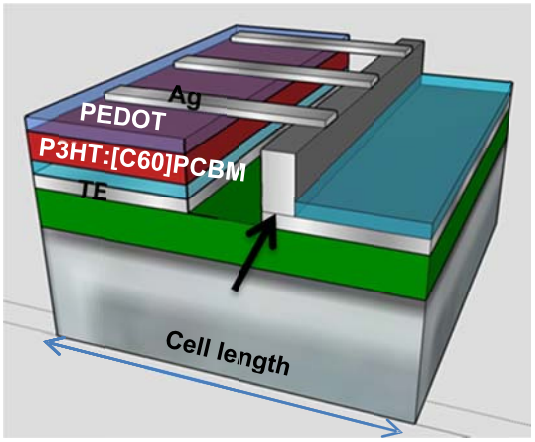

Figure 1: Schematic drawing of the device structure. Red: active layer, dark blue top: PEDOT layer, light blue bottom: electron transport/hole blocking layer (ETL/HBL); ignored in this calculation, gray bottom: TE back contact, gray top: metal fingers and interconnection. Green: isolation layer. Arrow indicates the area of contact between front and back contact

shunt resistance (R_{shunt}) and series resistance (R_{series}), a conducting top as defined by the PEDOT:PSS and a conducting bottom as defined by the backside TE contact. It is assumed that the ETL/HBL between the photo-active layer (here ZnO) and the TE contact is not contributing to the lateral transport and that its contribution to the resistance can be neglected. The voltage is applied to the TE contact at the right side of the device, while the TE edge on the left side is kept at 0V. The model then calculates the voltage distribution for a certain applied voltage using the Poisson equation for the metallization layers and the active layer. These layers are coupled via their contact resistance and diode properties. Iterations are done to make the voltages between the layers consistent. This is done for various applied voltages resulting in an I-V characteristics.

Cell size, interconnection area, finger length and width can be varied, as well as the material and diode parameters.

Table I: Parameter values used for the calculations of paragraph 2.2

Parameter	Value
sheet resistance metal (Ohm sq)	0.24 (=3xbulk Ag)
sheet resistance back (Ohm sq)	15
contact resistance finger/PEDOT (Ohm cm^2)	0.005
contact resistance in interconnect (Ohm cm^2)	0.005
rsheet pedot (Ohm sq)	500
thickness lines, back contact (mu)	0.2
fingerwidth (cm)	0.018
scribe widths (cm)	0.002
distance between scribes (cm)	0.006
distance between end finger/PEDOT (cm)	0.018
Jph (mA/cm^2)	10
n_{light}; n_{dark}	1.6; 1.3
J_{0light}; J_{0dark} (mA/cm^2)	8e-5;1.54e-6
$R_{shuntlight}$; $R_{shuntdark}$ (Ohm cm^2)	2000; 5e4

3 RESULTS

3.1 Cells having ITO and composite grid electrodes

Using the FEM model, calculations were performed for single cell modules, using typical parameters for P3HT:[C60]PCBM polymer solar cells as given in Table I. The grid width of 180 µm and 200 nm height were chosen as this can be easily printed using an inkjet printer. Higher lines up to 600 nm are possible but at reduced yield. The values for the diode parameters are based on experiments on P3HT:PCBM cells, where it was found that the diode parameters in the shaded regions under the metal have a different value than in the illuminated areas [13]. Fig. 2 shows the power density at maximum power point (Pmpp) for various finger pitches and scribe widths. As can be seen, the power first increases and then decreases with cell length. The initial increase is due to an increase in generated current density in the cell. For small device lengths, the active area is relatively small compared to the dead zone from the interconnection. Upon increasing the cell length, the active area increases and thus the current density and power increases. At increasing cell length, the electrical losses in the cell become more dominant and reduce the fill factor and open circuit voltage. Figure 2 shows that the optimal cell length is about 0.3 cm for cells with a

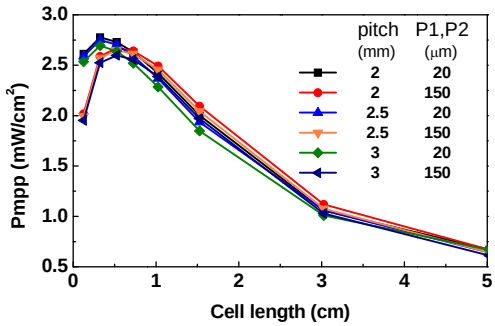

Figure 2: Power density at maximum power point (Pmpp) for varying scribe width (20, and 150 micron) and pitch (2-3 mm), where a metal resistance for the lines of 0.27 Ohm sq was used

scribe width of 20 micron and about 0.5 cm for cells with a scribe width of 150 micron. For the latter cells, the maximum power density is however slightly lower as the dead zone is larger. This only holds if the resistance in the interconnection is not limiting the module performance. If the scribe becomes so narrow that the contact resistance in the interconnect starts to play a role, the module efficiency will drop for narrower scribes. The largest generated power density is obtained for a cell with 20 micron P1 and P2 scribe width, a pitch of 2 mm and a cell length of 0.3 cm. To determine the major losses in the cell, the power dissipation is determined in the different parts of the cell. The result is shown in Fig.3. From this plot it can be concluded that the major loss at higher cell length is due to the high sheet resistance of the ITO back contact. This limits the cell length at optimal performance to about 0.3 cm.

The optimum cell length of 0.3 cm is rather small. Small cells require many interconnections per unit area, which means lower throughput in production. It seems more convenient to have larger cells. However, these cells will have a lower efficiency. Below a parameter

study is done to search for material parameters that would allow for a longer cell with minor loss in efficiency.

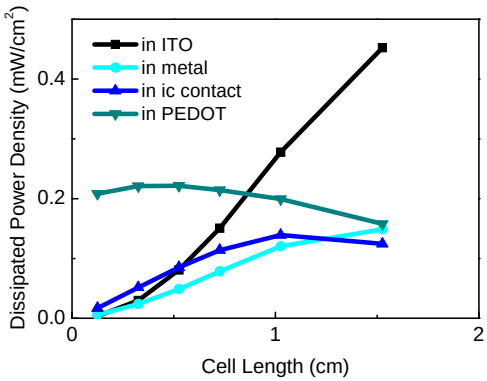

Figure 3: Dissipated power in different parts of the cell for a cell with 2 mm pitch and 20 micron P1 and P2 scribe width.

3.2 Cells containing a TE with lower sheet resistance

Figure 4 shows the results obtained using the typical material parameters, but reducing the sheet resistance for the backside TE from 15 Ohm sq (ITO) to 0.15 Ohm sq.

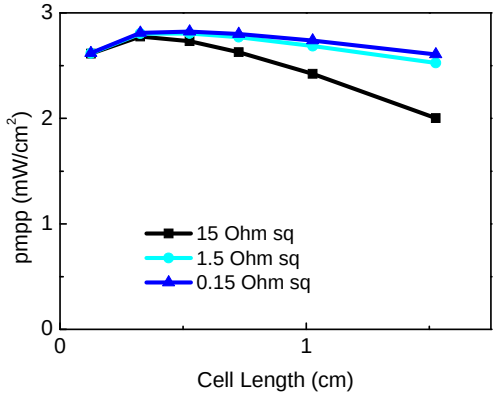

Figure 4: generated power density at maximum power point for a cell with 2 mm pitch and 20 micron P1 and P2 scribe width.

For a 10 times lower sheet resistance, the optimal cell length is at 0.7 cm. For a 100 times lower sheet resistance, the optimal cell length is also 0.7 cm and the maximum becomes much broader, but the performance only slightly higher. The lower sheet resistance can be obtained by replacing the ITO by a full area metal contact, while maintaining an IJP front contact. This allows for increased cell lengths up to roughly 1.5 cm.

3.3 Exploring parameter space for increased cell length

To further investigate the performance of cell with large cell length, the cell length was kept at 7 cm. This length was chosen as it would allow for a 2 cells interconnected module on our 6x6 inch substrates. For this cell length the sheet resistance of the metal grid and the contact resistance in the interconnection were reduced as well, see Fig. 5. The contact in the interconnect is shown in Fig.1 by the black arrow. It is the contact between the metal in the scribe and the backside contact. The pitch was kept constant at 2 mm in these calculations. As can be seen in Fig. 5, the Pmpp for a 7 cm long cell can be improved substantially when the metal line resistance is decreased a factor 10. However, this alone is not yet enough for efficient cells. Decreasing the contact resistance in the interconnection results in an additional increase in performance. Besides that also a reduction in the resistance of the back contact is needed.

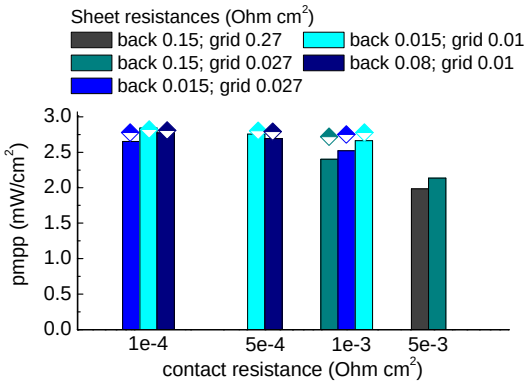

Figure 5: Pmpp for varying resistance values for a 7 cm long cell. Finger pitch is 2 mm.

These calculations show that quite some improvements are needed for polymer solar modules in order to maintain the efficiency at increased cell length. It also shows that resistance of the contact in the interconnect, of the back contact and of the metal grid all influence the performance of the module. This influence can be reduced if the current densities would be lower. Polymer tandem solar cells are currently made that have about half the current density of a single junction cell with twice the voltage. Figure 5 shows the effect on the Pmpp when the current density is reduced to half the current density of the single junction cell and the other cell parameters are adapted to reach a cell with twice the open circuit voltage (V_{oc}) and similar fill factor. The results are shown by the diamonds. As can be seen, the lower current density in these cells result in a higher Pmpp due to reduced resistance losses and the requirements on the sheet resistances are less stringent.

2.3 Calculation results for varying light intensity

As mentioned in the introduction, polymer solar cells will operate under various light conditions. It has been shown recently, that the light intensity behavior of P3HT:[C60]PCBM solar cells is accurately described by a 1-diode model with diode parameters that are light intensity dependent [14]:

$$\mathrm{Jph} = \mathrm{Jph0} * \mathrm{Ilight}$$

$$\mathrm{n} = \mathrm{nlow} + \frac{(\mathrm{nhigh} - \mathrm{nlow})}{(\mathrm{inthigh} - \mathrm{intlow})} * (\mathrm{Ilight} - \mathrm{intlow})$$

$$\mathrm{J_0} = \frac{\mathrm{Jph}}{e^{\left(\mathrm{Egap}*\frac{q}{n*k*T} - \frac{1.23}{n}\log\left(\frac{C}{\mathrm{Ilight}}\right)\right)} - 1}$$

$$\mathrm{Rshunt} = \frac{1}{\frac{1}{\mathrm{Rshuntlow}} + \frac{\left(\frac{1}{\mathrm{Rshunthigh}} - \frac{1}{\mathrm{Rshuntlow}}\right)}{(\mathrm{inthigh} - \mathrm{intlow})} * (\mathrm{Ilight} - \mathrm{intlow})}$$

Table II: Values for light intensity dependence of P3HT:[C60]PCBM diode parameters.

Parameter	Description	Value
J_{ph0}	Photon current density at 1 sun light intensity (mA/cm2)	6.135
I_{light}	Light intensity (number of suns)	0.13-1.0
n_{low}	Diode ideality factor at low light intensity	1.431
n_{high}	Diode ideality at high light intensity	1.673
Int_{high}	Light intensity at high light intensity (number of suns)	1.0
Int_{low}	Light intensity at low light intensity (number of suns)	0.13
E_{gap}	Bandgap energy	1.0
q	Elementary charge (C)	1.602e-19
k	Boltzmann constant (J/K)	1.381e-23
T	Temperature (K)	298.15
C	Fitting constant	3.9e6
$R_{shuntlow}$	Shunt resistance at low light intensity (Ohm cm2)	689.988
$R_{shunthigh}$	Shunt resistance at high light intensity (Ohm cm2)	6429.628

These light intensity dependent cell parameters were included in the model and calculations were done for light intensities varying from 0.2 to 1 sun. Table II gives the values for the diode parameters that were used in the calculation and Table III the values for the other parameters in the model. Note that the diode parameters used for these calculations differ from the ones used in the previous paragraphs.

Table III: Parameter values used for the calculations in paragraph 2.3

Parameter	Value
sheet resistance metal (Ohm sq)	0.2385 (=3 x bulk)
sheet resistance back contact (Ohm sq)	0.2385 (=3 x bulk)
contact resistance finger/PEDOT (Ohm cm2)	0.005
contact resistance in interconnect (Ohm cm2)	0.01
rsheet pedot (Ohm sq)	249.676
thickness lines, back contact (mu)	0.2
fingerwidth (cm)	0.01
scribe widths (cm)	0.002
distance between the scribes (cm)	0.01
distance between end finger and PEDOT (cm)	0.018

The resulting efficiency on total area is given in Fig. 6 for cell lengths of 1 and 2 cm and pitches of 1.5, 2 and 2.5 mm. For the 1 cm long device, the efficiency first increases with light intensity and then decreases for all pitches. Increasing the light intensity results in an increase in current density, which causes a decrease in fill factor due to resistive losses. On the other hand, the V_{oc} will increase with light intensity. These opposing mechanisms result in an optimum in efficiency around 0.5 sun. Increasing the cell length to 2 cm shifts the optimum to lower illumination intensity, as the resistive losses become larger, whereas the dependence of the V_{oc} on light intensity remains the same. Figure 6 also shows that the pitch can be optimized for light intensity. For the 2 cm long cell, the optimum pitch at 0.2 sun is 2.5 mm, whereas at 1 sun it is 1.5 mm. This clearly shows the need for optimization of grid patterns for different illumination intensities.

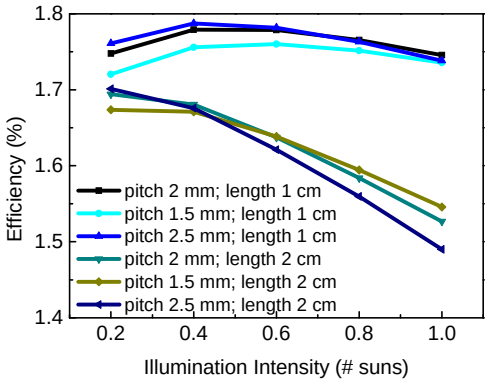

Figure 6: Efficiency versus illumination intensity for 1 and 2 cm long cells with 1.5, 2 or 2.5 mm pitch.

4 CONCLUSIONS

Using a FEM model with typical parameters for P3HT:[C60]PCBM solar cells, the cell length dependence was calculated. This resulted in an optimum length of about 0.5 cm. In order to investigate what is needed to increase the optimum length of a single cell in a module, a parameter study was performed, in which the cell length, interconnection area, contact resistance, finger line resistance, and resistance of the back contact were varied. It is found that for a backside sheet resistance of 0.08 Ohm sq, a contact resistance in the interconnection of 5e-4 Ohm cm^2 and a grid sheet resistance of the metal top grid of 0.01 Ohm sq, the cell length can be increased to 7 cm with only minor loss in efficiency. This would mean an increase in front side grid height from 200 nm to 4500 nm, based on a resistivity of 3 times the bulk resistivity for Ag. This cannot be done using ink jet printing, so screen printing and embedded grids must be used. If the contact resistance value of 5e-4 Ohm cm2 can be achieved depends on the materials of the top and bottom contact. If both materials are Ag this will probably not be a problem. The back side sheet resistance can be obtained by replacing ITO with a Ag sheet of 200 nm, or a similar PEDOT/Ag grid as the top metal grid. Further improvement in module efficiency can be obtained by going from a single to a tandem junction cell, where in general for tandems the current density is lower and the voltage higher than for the single junction. The dependency on material resistivity is therefore less strong, resulting in higher fill factors and consequently in higher module efficiencies.

The model also includes the light intensity dependence of the diode parameters assuming a 1-diode model for polymer solar cells. It is shown that the optimum pitch depends on both light intensity and cell length, indicating the need for metal grid optimization for different illumination conditions. With the presented model it is possible to optimize the design of thin film solar modules for use in various applications.

5 ACKNOWLEDGMENTS

This work has been supported by the European Commission as part of Framework 7 ICT 2009 collaborative projects HIFLEX (Grant no. 248678) and X10D (Grant no. 287818), and by the Dutch ministry of economic affairs through Agentschap NL within the project OZOFAB grant no. EOSLT1002. Tristran Budel is acknowledged for making the drawing for Fig. 1.

[1] M.A. Green, K. Emery, Y. Hishikawa, W. Warta, E.D. Dunlop, *Prog. Photovoltaics Res. Appl.* 20, 12 (2012).
[2] R.F. Service, Science, 332, 293 (2011).
[3] C. Lungenschmied, G. Dennlea, H. Neugebauer, S. N. Sariciftci, M. Glatthaarb, T. Meyer, A. Meyer, Solar Energy Materials & Solar Cells 91, 379 (2007).
[4] D. M. Tanenbaum, M. Hermenau, E. Voroshazi, M. T. Lloyd, Y. Galagan, B. Zimmermann, M. Hösel, H. F. Dam, M. Jørgensen, S. A. Gevorgyan, S. Kudret, W. Maes, L. Lutsen, D. Vanderzande, U. Würfel, R. Andriessen, R. Rösch, H. Hoppe, G. Teran-Escobar, M. Lira-Cantu, A. Rivaton, G. Y. Uzunoğlu, D. Germack, B. Andreasen, M. V. Madsen, K. Norrmany and F. C. Krebs, RSC Advances 2, 882 (2012).
[5] P. Schillinsky, C. Waldauf, J. Appl. Phys. 95, 2816 (2004).
[6] L.J.A. Koster, E. C. P. Smits, V. D. Mihailetchi, P.W. M. Blom, Phys. Rev. B 72, 085205 (2005).
[7] R. Häusermann, E. Knapp, M. Moos, N.A. Reinke, T. Flatz, B. Ruhstaller, J. Appl. Phys. 106, 104507 (2009).
[8] G-J. A. H. Wetzelaer, M. Kuik, M. Lenes, P.W. M. Blom, Appl. Phys. Lett. 99, 153506 (2011).
[9] G-J. A. H. Wetzelaer, M. Kuik, P.W. M. Blom, Adv. Energy Mater. 2, 1232 (2012).
[10] Y. Galagan, B. Zimmermann, E. W.C. Coenen, M. Jørgensen, D. M. Tanenbaum, F. C. Krebs, H. Gorter, S. Sabik, L. H. Slooff, S. C. Veenstra, J. M. Kroon, R. Andriessen, Adv. Energy Mater. 2, 103 (2012).
[11] B. Kippelen, S. Choi, W. J. Potscavage, 10th Int. Conf. NUSOD, 67, (2010).
[12] Y. Galagan, E. W.C. Coenen, B. Zimmermann, L. H. Slooff, W. J. H. Verhees, S. C. Veenstra, J. M. Kroon, M. Jørgensen, F. C. Krebs, R. Andriessen, accepted for publication in Advanced Energy Mat.
[13] L.H. Slooff, B. Brockholz, W.J.H. Verhees, S.C. Veenstra, E.M. Cobussen-Pool, J.M. Kroon and E.E. Bende, Energy Procedia 31, 11 (2012).
[14] L.H. Slooff, S.C. Veenstra, J.M. Kroon, W. Verhees, L.J.A. Koster, and Y. Galagan, tob e submitted to Solar En. Mater. & Solar Cells.